Published in final edited form as:
*J Vasc Interv Radiol*. 2009 October ; 20(10): 1343–1351. doi:10.1016/j.jvir.2009.05.038.

# Lethal isotherms of cryoablation in a phantom study: Effects of heat load, probe size and number

**Peter J. Littrup, M.D.**, **Bassel Jallad, M.D.**, **Vinaya Vorugu, M.D.**, **Gunnar Littrup**, **Brandt Currier**, **Michael George**, and **Donald Herring**
From the Karmanos Cancer Institute, Detroit, MI.

## Abstract

**Purpose—**The purpose of this study is to assess the effects upon lethal ice (< −30°C) proportions in different heat load phantoms while varying the size and number of cryoprobes at 2 cm spacing.

**Materials and Methods—**Thermocouples at 0.5, 1.0 and 1.5 cm intervals from 1.7 or 2.4 mm diameter cryoprobes were held by jigs accommodating 1–4 cryoprobes. Agar phantoms (N=24) used 3 sets of baseline temperatures at approximately 6°C, 24°C and 39°C. Temperatures during 15 minutes freeze cycles were correlated with actual thermocouple locations seen within the ice by computed tomography (CT). Diameters and surface areas of the −30°C lethal isotherm were assessed over time as percentages of the overall iceball.

**Results—**The high heat load, 39°C, phantom experiments showed the greatest impact upon percentage lethal zones for all probe configurations. Single, double, triple and quadruple probe arrangements of 2.4mm cryoprobes at 15 minutes had average lethal ice diameters of 1.2, 3.3, 4.1 and 4.9 cm, comprising 13 %, 46 %, 51 % and 56 % surface areas of lethal ice, respectively. Surface areas and diameters of lethal ice made by 1.7mm cryoprobes were 71%and 84% of the 2.4 mm cryoprobes, respectively. Lethal ice resides <1 cm behind the leading edge for nearly all probe configurations and heat loads.

**Conclusion—**Single cryoprobes have very low percentages of lethal ice. Multiple cryoprobes overcome both the high heat load of body temperature phantoms and help compensate for lower freeze capacity of thinner cryoprobes.

## INTRODUCTION

Cancer remains one of the leading causes of death in the USA with several challenges and complications involved in its treatment and management (1). Minimally invasive procedures like heat-based and cold-based ablations are gaining importance in the management of various types of tumors such as malignant tumors of the prostate (2), liver (3,4,5,6), kidney (7,8), lung (9) and larger benign breast tumors, such as fibroadenomas (10). Heat-based treatments, such as radiofrequency (RF) or microwave ablation, have dominated the early Interventional Oncology literature, however, measuring lethal tissue temperatures within an RF or microwave ablation zone requires expensive fiber-optic, non-metal thermocouples that don't distort the



**Please address all correspondences to:** Peter J. Littrup, MD, Department of Radiology, Karmanos Cancer Institute, 721 Harper Prof. Bldg., Detroit, Michigan 48201, (313) 576-9786 - Office, (313) 576-9960 – Fax, littrupp@karmanos.org.

energy fields or create their own heating focus when placed within the active heating zone. Reliable RF treatment zones have variable impedance during heating and are more unpredictable, especially near adjacent blood vessels (11) and in different tissue types or organs.

Cryoablation uses lethal cold temperatures of −20°C to −40°C depending upon the tissue type (12,13), and has been applied since 1845 (14). The modern era of percutaneous cryoablation began in the early 1980's when supercooled liquid nitrogen ($LN_2$) (Cryomedical Sciences, Inc., Kennesaw, GA) was pumped down cryoprobes as small as 3 mm in diameter. In the early 1990's, supercooled $LN_2$ was replaced by Joule-Thompson (JT) cooling which used rapid expansion of high pressure Argon gas for faster freezing and better control. However, probe power or wattage differences were never assessed, despite the extensive knowledge gained about cytotoxic zones around multiple cryoprobes within multiple organ systems (15–17), and particularly the prostate (18,19). More insight about these cytotoxic zones is needed for modern cryoprobes below 3mm in diameter, comparing single and multi-probe conditions in simple tissue-mimicking phantoms. Isotherm literature has been generated for computer modeling (17), room temperature phantoms (18,19), and normal animal tissues (15–16), but none used direct image correlations. Therefore, no guidelines exist for ultrasound (US) or computed tomography (CT) guided cryoablation that would help physicians appropriately plan cancer treatments based on tumor size.

We present the outcomes of freezing experiments using simple phantoms with variable heat loads, comparing thermocouple temperatures to their CT locations within the ice.

## Materials & Methods

No human or animal subjects, or tissues, were used during any portion of this study. No institutional review board was therefore needed for an in vitro phantom study. Parameters which could affect overall iceball size and underlying isotherms were limited for the scope of this study as noted below. Potential convective heat losses from blood flow were not addressed due to the complexities of simulating microvasculature. Agar phantoms of different temperatures mimicked different tissue heat loads. Underlying isotherms of each iceball were generated from thermocouple data and correlated with CT and US imaging over time. Descriptions below include phantom/procedure setup, cryoablation and imaging equipment, and finally imaging and data analyses.

### Agar phantoms

Four separate jigs were created to hold thermocouples and both the 1.7 and 2.4 mm cryoprobes in place for single, double, triple and quadruple multi-probe configurations using 2 cm spacing between all cryoprobes (figure 1a). All thermocouples measured temperature at their tip (Endocare Inc., Irvine CA) and were spaced 0.5, 1.0, and 1.5 cm from cryoprobes, as well as 0, 0.5, 1.0 and 1.5 cm along the line extending outward from the midpoint between 2 probes (Figure 1). The jigs were made of two identical pieces of wood, 5 × 18 × í inches screwed together with 1-inch thick spacers at each end to assure parallel spacing. Small silicon tubes were placed through the holes in each jig to assure that 1.7 or 2.4 mm cryoprobes and thermocouples would fit snugly and not move during testing.

Agar gel phantoms, which remain solid up to 60°C, were created from a 3% LB agar solution (Sigma-Aldrich Inc., St. Louis, MO) and then brought to the selected temperatures of approximately 6°C (refrigerator temperature = low heat load), 24°C (room temperature = medium heat load) and 39°C (near body temperature = high heat load). Phantoms were placed overnight in a patient blanket heater (Staris Corporation, Mentor, OH) to attain 39°C. No additional heating or cooling was done within the CT scanner to maintain their baseline

temperatures. A thermocouple was also placed into the periphery of agar phantoms to document the passive heating or cooling during each experiment. The tips of the thermocouples were placed approximately 1.5 cm from the distal tip of the cryoprobe to approximate the coldest region of the 4 cm active freeze segment. Prior to initiation of the freeze, the final position of cryoprobe and thermocouple distances were measured by both US and CT to correct for any displacement during insertion (figure 1a).

### Cryo-equipment and technique

Sharp-tipped cryoprobes (Endocare, Inc., Irvine, CA) with diameters of 1.7 and 2.4 mm were used for all freezing protocols. Cryoprobes were connected to a control unit with up to 8 ports (Endocare Inc., Irvine, CA) that regulated the flow of high-pressure argon gas. The JT cooling effect causes temperatures near the JT port to approach that of liquid Argon, or −187°C, however, actual temperatures at the probe surface vary between −130°C to −150°C due to individual probe variations and poor thermal conduction through argon gas within the expansion chamber to the outer metal sheath. Every freezing experiment included an initial freeze cycle of 15 minutes followed by a 5 minute passive thaw that only melts a few millimeters of the periphery (10). All thermocouple temperatures were recorded at 1 minute intervals for each freeze protocol. In order to limit CT time on our clinical scanner, a second freeze cycle of 10 minutes followed by another 5 minute passive thaw was only performed on the initial high heat load phantoms to save on CT scanner time constraints.

### Imaging equipment and protocols

Real-time US (GE Logiq 700 Milwaukee, Wisconsin) and CT (Siemens Somatom Plus4, Erlangen Germany) were used to measure the thermocouple locations in relation to the cryoprobe(s) within the agar phantoms. Measurements of the maximal diameter of the visualized ice ball were obtained at 1 minute intervals by US. However, US artifacts frequently degrade imaging after placement of more than one cryoprobe (8), and obscure thermocouple positions. In addition, US could not measure the posterior extent of ice due to a shadowing from the leading edge. Therefore, only CT images were used for measurements of probe/thermocouple locations inside the ice, as well as circumferential measurement of ice diameters. Due to X-ray tube cooling and imaging constraints, helical CT image acquisitions were obtained at 2 minute intervals. CT scanning obtained images with 5 mm slice thickness (280 mA and 120 kV) and covered up to 7 cm around the distal cryoprobe. Multiplanar CT reconstructions were used to estimate total iceball dimensions.

### Data and statistical analyses

Isotherm comparisons were done to assess qualitative differences in patterns of ice development. Excel spreadsheets (Microsoft Corp, Redmond, WA) were arranged to record ice sizes, cryoprobe/thermocouple distances, and temperatures over time for each freeze protocol. A total of 24 data sets were accumulated, encompassing 4 different probe configurations, within 3 different heat load phantoms, for both 1.7 and 2.4 mm cryoprobe sizes, each monitoring changes in temperature over time. CT Hounsfield units were also assessed for agar and ice over time.

The −30°C isotherm was chosen as the target temperature for potential cytotoxicity, since it conforms to clinical applications for cell death in nearly all tissues (12–19). Regression analyses of temperature vs. thermocouple distance from the cryoprobes allowed approximation of the −30°C isotherm. A regression, or trend line, was plotted from the CT-visible thermocouple distances from the cryoprobes and the resultant temperature noted over time. The distance from where the regression line crossed the −30°C line was used for the isotherm distance inside the ice margin at that time point. Separate regression lines were obtained for the 3 thermocouples placed 0.5, 1.0, and 1.5 cm directly adjacent to a cryoprobe, as well as the

4 thermocouples placed 0, 0.5, 1.0, and 1.5 cm extending outward along the line equidistant between any 2 cryoprobes (Figure 1). Isotherm figures were then generated for each of the 24 experimental conditions showing the final ice size and the −30°C isotherm at the conclusion of the 15 minute freeze, as well as the progression of the lethal isotherm at 5, 10, and 15 minutes (17). The diameter and surface area at the level of the recorded thermocouple tips was chosen over volume calculations to avoid any inaccuracies related to approximations of additional isotherms in the longitudinal direction. After the isotherms began to fuse at approximately 5 minutes, the surface area calculations became irregular, until synergy between cryoprobes caused smoothing of these underlying isotherms into simpler geometric shapes by approximately 10 minutes. Therefore, surface area measurements from 10 minutes and 15 minutes allowed geometric calculations of the surface area of the lethal ice for probe and phantom load comparisons.

Statistical analyses were limited to descriptive observations of qualitative differences in overall ice size and associated isotherm shape and size, not intended to power the sample size of the study. Analyses were limited to differences in diameter and cross-sectional surface area and not volume, due to the uncertainty of both imaging and thermocouple measurements in the length axis of the iceball. Accuracy of the isotherm locations within the iceball was estimated from the greatest potential error in distance where the regression line crossed the −;30° C. Similarly, isotherms over time (17) were only intended to graphically display the effects of heat load, probe size, and configuration differences.

## Results

Overall experiment observations are noted first. The construction of simple wooden jigs allowed reproducible data gathering, despite the inconvenience of the agar phantoms. CT provided circumferential imaging of the iceball, as well as the exact location of the internal thermocouples relative to their respective cryoprobes. Our data demonstrated that more than one cryoprobe created thermal synergy by pushing the lethal isotherm further out between the cryoprobes than radially outward from individual cryoprobes, once the lethal isotherms had fused between 5 and 10 minutes. The percentage of iceball surface area ≤−30°C was dependent upon the relative heat load of the phantoms, the number in diameter of the cryoprobes.

A total of 4056 individual temperature measurements were collected over 24 experiments. Table 1 shows the absolute and percentage of lethal ice for all 24 experiments. Technical malfunctions (e.g., thermocouple readings) in isotherm calculations were only noted for the single 2.4 mm cryoprobe in the cold phantom and the triple 2.4 mm cryoprobe configuration in the warm phantom. Otherwise, table 1 shows a consistent trend toward lower percentages of lethal ice for higher heat load phantoms and fewer cryoprobes. The cytotoxic margin remains consistent at approximately 1 cm behind the leading edge of ice, yet trended toward narrower non-lethal margins for higher heat loads and greater freeze capacity (e.g., quadruple 2.4 mm cryoprobes). While no comparative regression statistics were performed on this small sample size, isotherms were visually approximated to be accurate ± 1 mm. Therefore, the ratios of the iceball surface areas for the −30°C and 0°C isotherms produced accurate qualitative estimates of the cytotoxic zone and total iceball sizes over time.

Figure 1 demonstrates that CT images were able to account for minor variations in thermocouple distance from the cryoprobe, encountered during insertion into the agar despite the fixation jigs. The minimal effect of the thaw and re-freeze phases (figure 1 b/c) suggested little role for phantom testing since there is no physiologic warming during the thaw phase (10), which is crucial for lethal osmotic effects in living tissue (12,13). Within three minutes of initiating the re-freeze, all thermocouples appeared to resume the same freeze rate they had at the conclusion of the first 15 minute freeze cycle. Since no additional information would be

gained from a second freeze in relation to isotherm patterns, they were discontinued for the remainder of the experiments.

Figure 2 graphically demonstrates the effects of greater heat load, particularly for single 1.7 mm cryoprobes, which is overcome by multiple cryoprobes (table 1). Figure 3 graphically shows the overall ice and lethal zone ratios between 1.7 and 2.4 mm cryoprobes in the high heat load phantoms. Figure 4 graphically shows that the overall concept of sculpting a lethal isotherm related to probe number, size and total freeze time. Similar ice sizes and lethal zones were achieved by a *double* configuration of 2.4 mm cryoprobes at 15 minutes, a *triple* configuration of 1.7 mm cryoprobes at 15 minutes, or a *triple* configuration of 2.4 mm cryoprobes for only 10 minutes. However, rapid freeze rates are more cytotoxic (12,13), such that the largest freeze within the shortest time would favor using more cryoprobes until more powerful cryoprobes become available. Figure 5 emphasizes the impacts of cryoprobe differences over time in higher heat load phantoms. At 5 minutes, the lethal zones of the 2.4 mm cryoprobes had fused and produced thermal synergy that caused even larger cytotoxic isotherms by 10 and 15 minutes for both 2 and three-probe configurations.

## DISCUSSION

The overall iceball diameter of a single cryoprobe, produced within room temperature or refrigerated phantoms, is often quoted as a surrogate of freeze capacity but is a misleading estimate of crucial isotherms within an iceball, generated in a body temperature volume Unfortunately, single iceball estimates have served as sales and marketing claims to suggest better ablation performance for one brand, or cryoprobe type, than another. Regardless of these assertions, a cryoprobe of nearly any size or power would form little to no ice if held under the large heat sink of warm running water. The focus upon total ice ball size, rather than the percentage of lethal ice, may also stem from ice being visible by nearly any imaging modality. What was thus an imaging benefit of cryoablation may have also led to misconceptions about the bio-physics of ice formation around a cryoprobe and neglected cryobiology principles necessary for lethal ice formation and cytotoxic cancer therapy. Our simplistic and limited evaluation of isotherm effects from variable heat loads, multiple cryoprobes and potential power differences between probe sizes may lead to more in-depth studies regarding these considerations in planning effective cryoablations.

Treatment planning and control of ablation margins by cryoablation is facilitated by CT imaging showing low density regions growing around cryoprobes (5,7–9), or the advancing hyperechoic rim of ice by US (2,6,10). However, the edge of visible ice at 0°C is usually at least 5mm ahead of the underlying lethal isotherm (12,13) when using multiple cryoprobes, and the outcomes of our study confirm that this non-lethal margin is consistently less than 1 cm (table 1). We demonstrated the cumulative effects of multiple cryoprobes upon the percentage of ice occupied by lethal temperatures below −30°C (figure 3), including the ability of multiple probes to overcome the effects of increased heat load (figure 2). Our qualitative outcomes show the impact of probe number and strength upon isotherms over time (figure 4,5), especially under higher heat load conditions. Further assessment of isotherm patterns with simulated vasculature [e.g., urethral warming balloon (18,19)] will allow more reproducible planning of cytotoxic tissue temperatures for nearly any cryoablation procedure.

Our data applies to all percutaneous cryoablation procedures for tumors <4 cm in diameter but could be expanded to even larger tumors by using more than 4 cryoprobes. However, the greatest clinical impact in better understanding of cytotoxic isotherm patterns for 1–4 cryoprobes may be for breast cancer ablation trials that have routinely used single cryoprobe treatments (23–26). Unfortunately, the upcoming trial of the American College of Surgeons Oncology Group (ACOSOG) using only 1 cryoprobe for breast tumors <1.5 cm in diameter

may yield suboptimal outcomes due to inadequate isotherms (27). The transition of breast cryoablation from benign to malignant disease will require ablation zones of visible ice extending >1 cm beyond all tumor margins, thus mimicking standard "surgical" margins. A 3 cm diameter zone of *lethal* temperatures would thus be needed to cover a 1.5 cm breast cancer, as suggested by the cryoprobe options noted in figure 4. To better cover the spherical shape of most tumors, cryoprobe selection may favor at least three cryoprobes to produce a more symmetric coverage since the double 2.4 mm configuration produces more ovoid ice with an average AP lethal zone of only 2.5 cm at the conclusion of a 15 minute freeze cycle. Therefore, if puncture risk is not an issue, using three 2.4 mm cryoprobes to generate the same amount of lethal ice at 10 minutes would produce faster freeze rates associated with greater cytotoxicity (12,13). Faster freeze rates have also been described by closer spacing of cryoprobes (18,19) than the 2 cm noted for this study and others (15).

Multiple cryoprobes, thermocouples, and subsequent ice formation produced major US artifacts that precluded reliable US measurements for this study. US imaging for cryoablation remains a valuable guidance tool for prostate cancer (2) and benign breast tumors (10) but only produces visualization of the leading edge of the overall iceball for those applications. Our study confirmed that CT imaging better defined the circumferential extent of all iceballs and was not significantly obscured by beam hardening artifacts from the multiple cryoprobes and thermocouples. Even in our highest heat load phantoms, lethal ice diameters up to 5 cm could be produced for quadruple configurations of both 1.7 and 2.4 mm cryoprobes. Nevertheless, these body temperature phantoms still appeared to only mimic live tissue that has relatively low blood flow and/or good thermal conductivity. Namely, when a similar spacing of 2 cm between 2.4 mm cryoprobes was used in porcine liver and lung cryoablation, cytotoxic temperatures were not reached between probes at 10 minutes (15). This may have related more to the thermal conductivity of the liver and lung tissue than any exceptionally high heat load since their renal cryoablation experiments (i.e., high blood flow organ) showed fusion of cytotoxic isotherms by 10 minutes. Therefore, our body temperature phantoms may better mimic the good thermal conductivity of renal tissue since our multi-probe configurations showed fusion of cytotoxic isotherms around the individual cryoprobes at 5–10 minutes (figure 5), whereas in vivo lung and liver tissue may not have similar thermal conductivity.

A large amount of thermal and imaging data was gathered for this study, yet numerous potential weaknesses limit more precise characterizations of 1.7 and 2.4 mm cryoprobe performances. Agar phantoms used in this study allowed heating to body temperature but did not sufficiently estimate the thermoregulation of living tissues, leading us to terminate data collection during the second freeze since these were non-physiologic. The study was only designed to produce insights for clinical technique modifications in relation to cryoprobe number, power and relative heat load effects for 2 cm spacing between cryoprobes. Further work is needed to also define the isotherm effects of cryoprobe spacing at 1.0 and 1.5 cm, but should *not* be explored for >2.0 cm spacing since this does not produce lethal ice between probes in normal liver and lung (15). More powerful cryotechnology (28) may allow greater spacing, or at least faster attainment of cytotoxic treatment goals.

The multi-probe configurations used in this study were also limited by the simple construction of the wooden jigs that held both 1.7 and 2.4 mm cryoprobes. Thermocouples and cryoprobes were both noted to move during insertion into some agar phantoms. However, CT measurements accounted for these deviations in the development of the lethal isotherm lines. Additional jigs will also be needed to evaluate the effects of additional cryoprobe spacing (17), as well as adding an additional heat sink to mimic adjacent vasculature. Lethal isotherms were only given in diameter and surface area measurements. Further volumetric isotherms will have to be constructed from temperature data collected along the long axis of the cryoprobe, requiring thermocouples with multiple measurement points along their longitudinal course and

connected to a digital acquisition device having at least 16 ports. More temperature data points and a volumetric rendering program (e.g., Comsol, Burlington MA) would also better define the changing size of the lethal isotherm volumes over time, which we limited in this current study to 5, 10 and 15 minutes when they had simpler geometric shapes. In the future, individual cryoprobe power also needs to be directly measured in wattages, whereby an electric heater and a thermocouple covers the cryoprobe tip, such that heating can be increased until no ice (0°C) is formed around the cryoprobe within an isolated, or near vacuum, container. The point at which heater overcomes ice formation would then describe a reliable wattage, or objective power, of that probe.

Isotherm research is well suited for cryoablation investigations since the ablation zone is clearly visualized and temperatures are easily measured, especially with the aid of CT guidance. Our paper provides a simple methodology for assessing the concepts of sculpting lethal isotherms. Probe synergy between multiple cryoprobes allows the lethal ice diameter of single cryoprobes to increase from approximately 35% to >70% for three or more cryoprobes, while maintaining a <1 cm non-lethal margin from the leading edge of visible ice (e.g., 0°C). Reliable testing models that better mimic the heat loads of living tissue will advance isotherm research and help answer important questions about cryotechnology performance and its role in the continued growth of interventional oncology.

## Acknowledgments

All authors wish to thank the lead CT technician, Folorunsho Ayo Kufeji, for his dedication, volunteered time and inspiration.

## REFERENCES

1. Jemal A, Siegel R, Ward E, Hao Y, Xu J, Murray T, Thun MJ. Cancer statistics, 2008. CA Cancer J Clin 2008;58:71–96. [PubMed: 18287387]
2. Bahn DK, Lee F, Badalament R, Kumar A, Greski J, Chernick M. Targeted cryoablation of the prostate: 7-year outcomes in the primary treatment of prostate cancer. Urology 2002;60:3–11. [PubMed: 12206842]
3. Tateishi R, Shiina S, Teratani T, et al. Percutaneous radiofrequency ablation for hepatocellular carcinoma. An analysis of 1000 cases. Cancer 2005;103:1201–1209. [PubMed: 15690326]
4. Joosten J, Jager G, Oyen W, Wobbes T, Ruers T. Cryosurgery and radiofrequency ablation for unresectable colorectal liver metastases. Eur J Surg Oncol 2005;32:1152–1159. [PubMed: 16126363]
5. Lee FT Jr, Chosy SG, Littrup PJ, Warner TF, Kuhlman JE, Mahvi DM. CT-monitored percutaneous cryoablation in a pig liver model: pilot study. Radiology 1999;211:687–692. [PubMed: 10352592]
6. Kerkar S, Carlin AM, Sohn RL, et al. Long-term follow up and prognostic factors for cryoablation of malignant liver tumors. Surgery 2004;136:770–779. [PubMed: 15467661]
7. Allaf ME, Varkarakis IM, Bhayani SB, Inagaki T, Kavoussi LR, Solomon SB. Pain control requirements for percutaneous ablation of renal tumors: cryoablation versus radiofrequency ablation--initial observations. Radiology 2005;237:366–370. [PubMed: 16126920]
8. Littrup P, Ahmed A, Aoun H, et al. CT-guided percutaneous cryotherapy of renal masses. J Vasc Interv Radiol 2007;18:383–392. [PubMed: 17377184]
9. Wang H, Littrup PJ, Duan Y, Zhang Y, Feng H, Nie Z. Thoracic masses treated with percutaneous cryoablation: initial experience with more than 200 procedures. Radiology 2005;235:289–298. [PubMed: 15798173]
10. Littrup PJ, Freeman-Gibb L, Andea A, White M, Amerikia KC, Bouwman D, Harb T, Sakr W. Cryoablation for breast fibroadenomas. Radiology 2005;234:63–72. [PubMed: 15550369]
11. Lu DS, Raman SS, Limanond P, Aziz D, Economou J, Busuttil R, Sayre J. Influence of large peritumoral vessels on outcome of radiofrequency ablation of liver tumors. J Vasc Interv Radiol 2003;14:1267–1274. [PubMed: 14551273]

12. Gage AA, Baust J. Mechanisms of tissue injury in cryosurgery. Cryobiology 1998;37:171–186. [PubMed: 9787063]
13. Hoffmann NE, Bischof JC. The cryobiology of cryosurgical injury. Urology 2002;60:40–49. [PubMed: 12206847]
14. Gage AA. History of cryosurgery. Semin Surg Oncol 1998;14:99–109. [PubMed: 9492880]
15. Permpongkosol S, Nicol TL, Khurana H, et al. Thermal maps around two adjacent cryoprobes creating overlapping ablations in porcine liver, lung and kidney. Journal of Vascular and Interventional Radiology 2007;18:283–287. [PubMed: 17327563]
16. Permpongkosol S, Nicol TL, Khurana H, et al. Differences in ablation size in porcine kidney, liver, and lung after cryoablation using the same ablation protocol. AJR Am J Roentgenol 2007;188:1028–1032. [PubMed: 17377040]
17. Berger WK, Poledna J. New strategies for the placement of cryoprobes in malignant tumors of the liver for reducing the probability of recurrences after hepatic cryosurgery. Int J Colorectal Dis 2001;16:331–339. [PubMed: 11686533]
18. Rewcastle JC, Sandison GA, Muldrew K, Saliken JC, Donnelly BJ. A model for the time dependent three-dimensional thermal distribution within iceballs surrounding multiple cryoprobes. Med Phys 2001;28:1125–1137. [PubMed: 11439482]
19. Baissalov R, Sandison GA, Donnelly BJ, et al. A semi-empirical treatment planning model for optimization of multiprobe cryosurgery. Phys Med Biol 2000;45:1085–1098. [PubMed: 10843092]
20. Evans W, Fish J, Keblinski P. Thermal conductivity of ordered molecular water. J Chem Phys 2007;126:154504. [PubMed: 17461644]
21. Gupta A, Allaf ME, Kavoussi LR, et al. Computerized tomography guided percutaneous renal cryoablation with the patient under conscious sedation: initial clinical experience. J Urol 2006;175:447–452. [PubMed: 16406968]
22. Gill IS, Remer EM, Hasan WA, et al. Renal cryoablation: outcome at 3 years. J Urol 173:1903–1907. [PubMed: 15879772]205
23. Pfleiderer SO, Freesmeyer MG, Marx C, Kuhne-Heid R, Schneider A, Kaiser WA. Cryoablation of breast cancer under ultrasound guidance: initial results and limitations. Eur Radiol 2002;12:3009–3014. [PubMed: 12439583]
24. Roubidoux MA, Sabel MS, Bailey JE, Kleer CG, Klein KA, Helvie MA. Small (< 2.0-cm) breast cancers: mammographic and US findings at US-guided cryoablation--initial experience. Radiology 2004;233:857–867. [PubMed: 15567802]
25. Pfleiderer SO, Marx C, Camara O, Gajda M, Kaiser WA. Ultrasound-guided, percutaneous cryoablation of small (< or = 15 mm) breast cancers. Invest Radiol 2005;40:472–477. [PubMed: 15973140]
26. Pusztaszeri M, Vlastos G, Kinkel K, Pelte MF. Histopathological study of breast cancer and normal breast tissue after magnetic resonance-guided cryoablation ablation. Cryobiology 2007;55:44–51. [PubMed: 17604016]
27. Kaufman, C. Cryoablation - The Next Advance in Breast Cancer Care?. www.touchbriefings.com/pdf/1438/ACF53E.pdf
28. Littrup, PJ.; Babkin, AV.; Duncan, R.; Boldarov, S. Cryoablation System. US patent. #7,083,612. Issued August 1, 2006

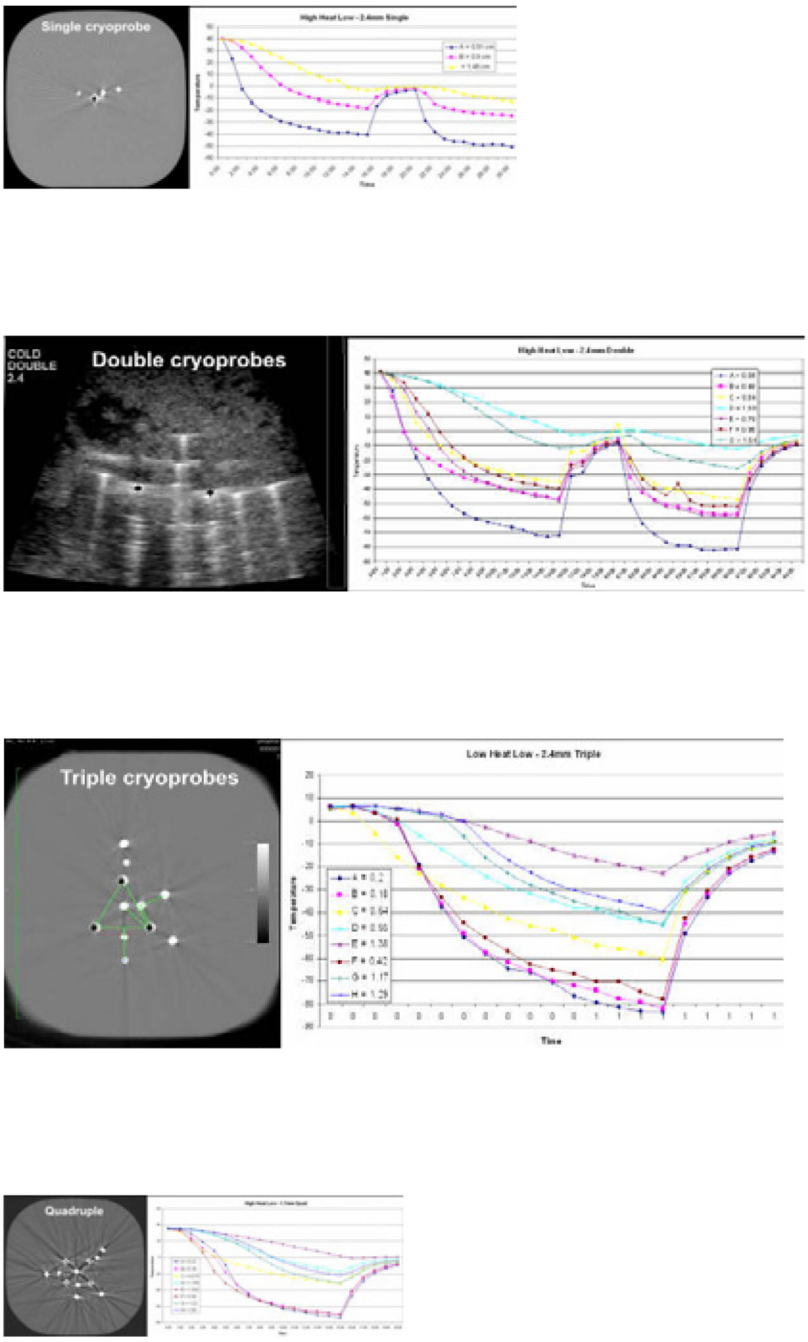


**Figure 1.**
Phantom set up within CT scanner gantry (a) and associated images of the single (b), double (c), triple (d) and quadruple cryoprobe (e) arrangements showing thermocouples radially surrounding the cryoprobes at 0.5 1.0 and 1.5 cm, as well as extending outward along a perpendicular line between the cryoprobes. Companion temperature graphs are shown for each configuration but only the single and double are shown with a freeze:thaw:freeze cycle obtained in the highest heat load phantoms (39°C). Despite the lack of any physiologic warming during the thaw phase, temperature curves still show rapid re-cooling of the ablation volume due to the 4-fold greater conductivity of ice during the second freeze (20).

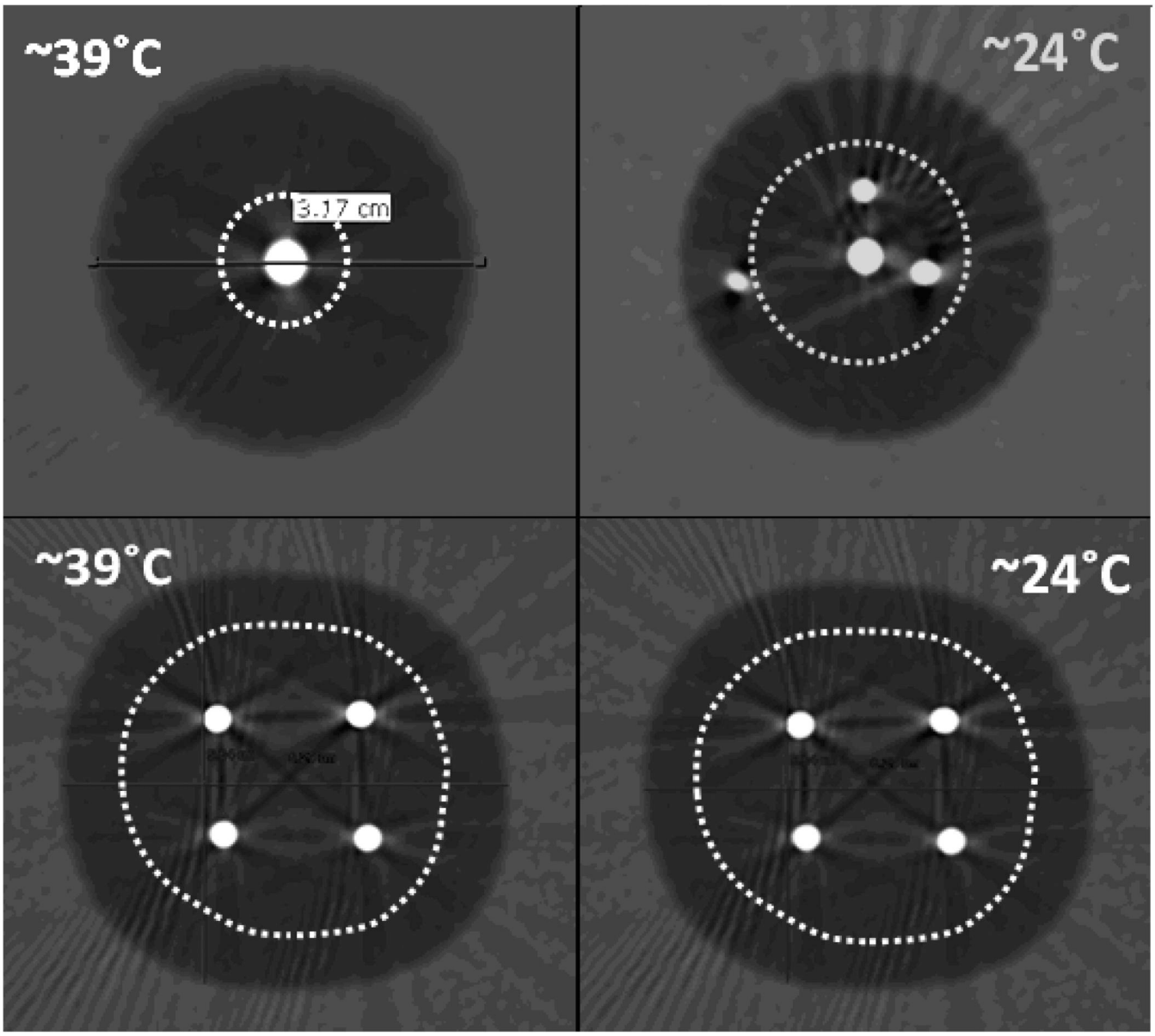


**Figure 2.**

*Heat load*: 1.7 mm cryoprobes at 15 minutes showing the slightly greater impact of high heat load (39°C) upon smaller cryoprobes and the compensatory effect of multi-probes. The overall ice had 1.6 times greater cross-sectional surface area for the 24°C medium heat load phantom (12.0 versus 7.6 $cm^2$; Diameter = 3.1 vs. 3.9), but the lethal zone was three times larger (2.7 versus 0.9 $cm^2$; Diameter = 1.1 vs. 1.9). These differences are overcome with four cryoprobes, whereby the surface area ratios of total/lethal ice for the high and medium heat load phantoms are 29.2/15.2 $cm^2$ (diam: 6.5/4.9 cm) and 31.3/14.9 $cm^2$ (diam: 6.7/5.0 cm), respectively.

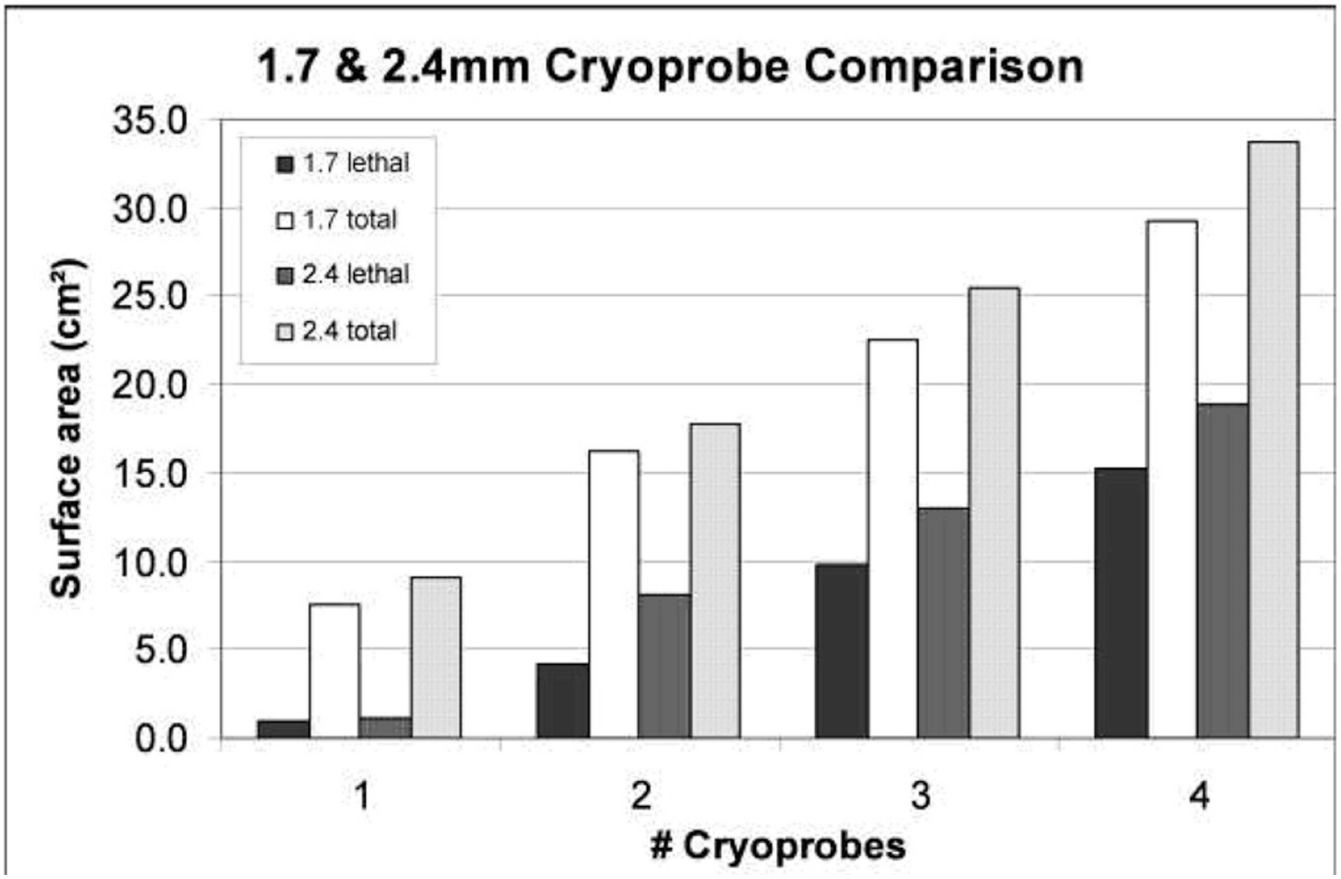


**Figure 3.**
The greatest increase in lethal ice percentage for either 1.7 or 2.4 mm cryoprobes is obtained when adding the second cryoprobe. Continued large increase in lethal ice is also seen when the third 1.7 mm cryoprobe is adding, suggesting also their weaker freeze capacity.

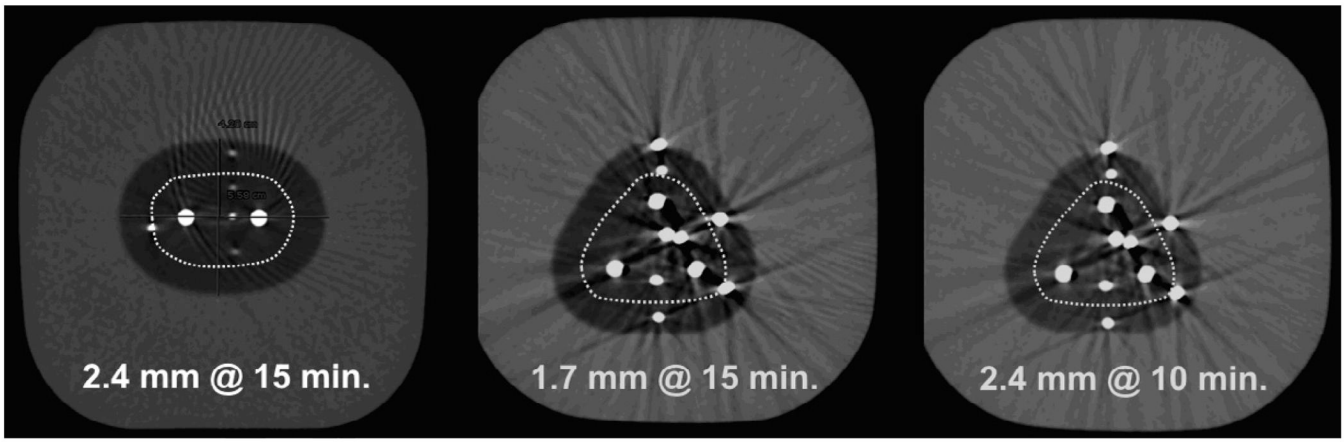


**Figure 4.**
Time and probe number options are shown that could conceivably cover a ~1 cm irregular tumor with a generous 3 cm diameter lethal ice ablation zone. A double 2.4 mm cryoprobe configuration ran to its longest practical extent at ~15 minutes produces similar overall ice and lethal zone as a triple configuration of 1.7 mm cryoprobes at 15 minutes, or triple 2.4 mm probes run for only 10 minutes.

| A | B | C |
|---|---|---|
| Double 2.4 mm@15 min. | Triple 1.7 mm @ 15 min. | Triple 2.4 mm @ 10 min. |
| Total ice ($cm^2$): 17.7 | 22.6 | 19.9 |
| Lethal ice ($cm^2$): 8.1 | 9.9 | 9.0 |
| Lethal diam. (cm): 3.3 | 3.5 | 3.4 |

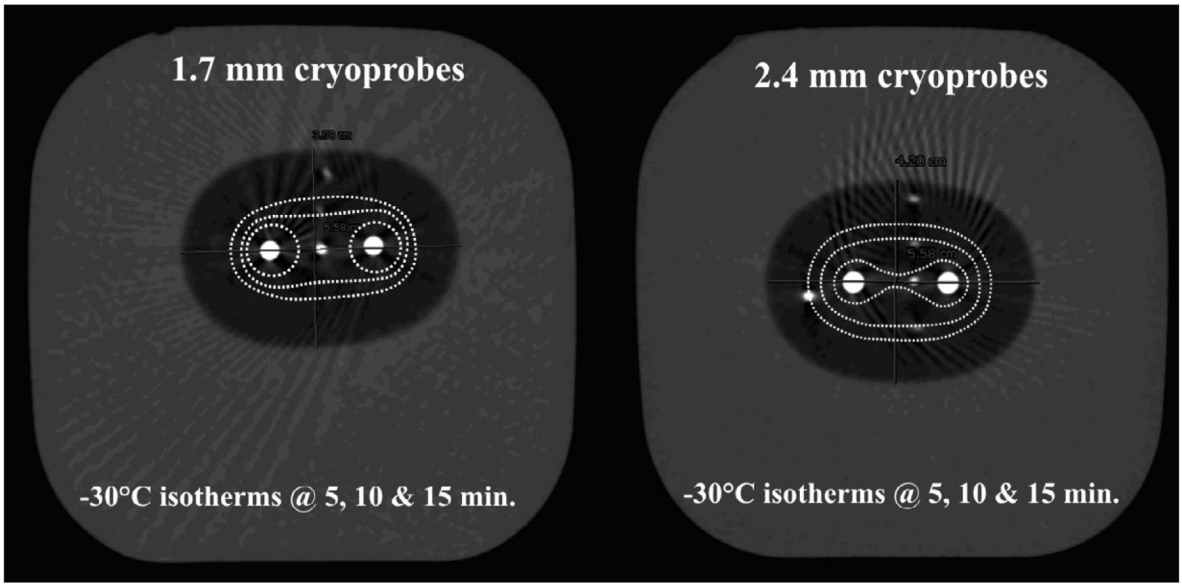


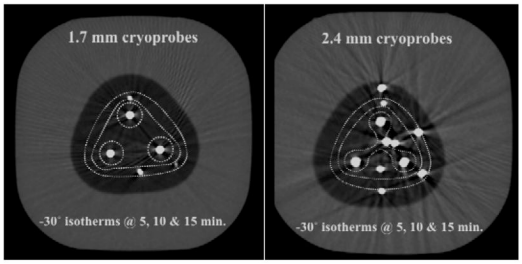


**Figure 5.**
Progression of the lethal isotherm (−30°C) at 5 (dashed white lines), 10 (dashed pink lines) and 15 (dashed red lines) minutes is shown for double and triple configurations of 1.7 and 2.4 mm cryoprobes, overlaid upon the CT image for the total ice appearance at 15 minutes. Figure 5a shows that lethal ice surface area grows more for 2.4mm cryoprobes (right) after 5 minutes due to early synergy than for 1.7 mm cryoprobes (left):

| ***Lethal zones:*** **1.7 mm cryoprobes** ($cm^2$) | **2.4 mm cryoprobes** ($cm^2$) | |
|---|---|---|
| 1.0 | 1.1 | 5 min. |
| 2.5 | 5.6 | 10 min. |
| 4.1 | 8.1 | 15 min. |

Figure 5b shows that lethal ice surface area grows more for 2.4mm cryoprobes (right) after 5 minutes due to early synergy but the difference becomes less over time once synergy also occurs for 1.7 mm cryoprobes (left):

| *Lethal zones:* 1.7 mm cryoprobes ($cm^2$) | 2.4 mm cryoprobes ($cm^2$) | |
|---|---|---|
| 1.3 | 3.4 | 5 min. |
| 7.0 | 9.0 | 10 min. |
| 9.9 | 13.0 | 15 min. |

**Table 1**

Absolute and percentage measurements of total and lethal ice are given for data sets from in vitro phantoms having in three different temperatures, according to number and diameter of cryoprobes. Note the probable thermocouple error and the resultant disproportionately small lethal ice measurements for the 2.4 mm cryoprobe data sets in the single "low" and triple "medium" data sets (*), since the total ice size by CT appears appropriate..

| | | Phantom Temperature (heat load) | | | | |
|---|---|---|---|---|---|---|
| Number of Cryoprobe | Cryoprobe Diameter (mm) | Average Diameter (cm) | | Diameter %Lethal | Non-Lethal | Surface Area |
| | | Iceball | Lethal Zone | | Margin (cm) | %Lethal |
| | | Low (6°C) | | | | |
| 1 | 1.7 | 4.4 | 2.3 | 52% | 1.1 | 27% |
| | 2.4 | 4.4 | 1.3 | 30% | 1.6 | 9% |
| 2 | 1.7 | 5.4 | 3.1 | 58% | 1.1 | 33% |
| | 2.4 | 5.8 | 3.8 | 66% | 1.0 | 43% |
| 3 | 1.7 | 6.5 | 3.9 | 61% | 1.3 | 37% |
| | 2.4 | 6.9 | 4.6 | 66% | 1.2 | 44% |
| 4 | 1.7 | 6.9 | 4.6 | 67% | 1.1 | 45% |
| | 2.4 | 7.5 | 6.5 | 87% | 0.5 | 76% |
| | | **Medium (24°C)** | | | | |
| 1 | 1.7 | 3.9 | 1.9 | 48% | 1.0 | 23% |
| | 2.4 | 4.0 | 1.9 | 48% | 1.1 | 23% |
| 2 | 1.7 | 4.5 | 2.4 | 54% | 1.0 | 24% |
| | 2.4 | 5.1 | 3.2 | 62% | 1.0 | 38% |
| 3 | 1.7 | 6.3 | 4.0 | 64% | 1.1 | 41% |
| | 2.4 | 6.1 | 3.4 | 56% | 1.3 | 31% |
| 4 | 1.7 | 6.3 | 4.4 | 69% | 1.0 | 48% |
| | 2.4 | 6.8 | 5.0 | 74% | 0.9 | 55% |
| | | **High (39°C)** | | | | |
| 1 | 1.7 | 3.1 | 1.1 | 35% | 1.0 | 12% |
| | 2.4 | 3.4 | 1.2 | 36% | 1.1 | 13% |
| 2 | 1.7 | 4.6 | 2.4 | 52% | 1.1 | 25% |
| | 2.4 | 4.8 | 3.3 | 69% | 0.7 | 46% |
| 3 | 1.7 | 5.4 | 3.6 | 66% | 0.9 | 44% |

| | | | Phantom Temperature (heat load) | | | | | |
|---|---|---|---|---|---|---|---|---|
| | | | Average Diameter (cm) | | | Non-Lethal | Surface Area |
| Number of Cryoprobe | Cryoprobe Diameter (mm) | | Iceball | Lethal Zone | Diameter %Lethal | Margin (cm) | %Lethal |
| 4 | 2.4 | | 5.7 | 4.1 | 72% | 0.8 | 51% |
| | 1.7 | | 6.1 | 4.4 | 72% | 0.9 | 52% |
| | 2.4 | | 6.6 | 4.9 | 75% | 0.8 | 56% |